

Seismic Responses of Masonry Structures Strengthened with FRP Laminates: a Shaking-table Study

Li-hua Xu, Si Zhang, Xiao-bin Hu & Ming-jie Zhang

School of Civil Engineering, Wuhan University, China

Li-hua Xu, Si Zhang, Xiao-bin Hu & Ming-jie Zhang

Hubei Provincial Key Laboratory of Geotechnical and Structural Engineering Safety, Wuhan University, China



SUMMARY:

To compare the seismic performance of masonry structures strengthened with different Fiber Reinforced Plastic (FRP) laminates under three different earthquake records, shaking table tests of two 1/4 scaled two-bay and two-storey masonry structures strengthened with Carbon Fiber Reinforced Plastic (CFRP) and Basalt Fiber Reinforced Plastic (BFRP) laminates respectively were conducted. It was observed that the BFRP-strengthened specimen was damaged more severely, although the two specimens exhibited similar damage pattern. BFRP-strengthened specimen yielded larger acceleration response than the CFRP-strengthened one and was more sensitive to the variation of earthquake record. Torsion was observed in both specimens, which was more obvious in the BFRP-strengthened specimen. The measured strain on the laminates showed that the BFRP and CFRP have similar mechanism of reinforcing the masonry structures. It was concluded that the masonry structures strengthened with CFRP or BFRP laminates had comparable seismic performance, while BFRP laminates were relatively cheaper.

Keywords: masonry structure; CFRP; BFRP; seismic response; shaking table test

1. INSTRUCTION

Masonry structure is one of the most common structure types; however, due to its low strength, heavy weight and poor stability, masonry structures often experience severe damages under seismic excitations. At present, numerous existing masonry buildings in China need to be repaired due to no conducting seismic design or the requirements of seismic upgrade. Currently, Fiber Reinforced Plastic (FRP) has attracted a lot of attention in the engineering practice of reinforcing masonry buildings due to its lightweight, high strength, corrosion resistance and no impact on the shapes of the structures. FRP materials mainly include Glass Fiber Reinforced Plastic (GFRP), Aramid Fiber Reinforced Plastic (AFRP), Carbon Fiber Reinforced Plastic (CFRP) and Basalt Fiber Reinforced Plastic (BFRP), among which CFRP gains the most popularity for its good mechanical and physics characteristics. Compared with CFRP, the tensile strength and elastic modulus of BFRP are relatively lower; however, its price is lower, which may make it an appealing retrofitting measure for the masonry structures.

In the late 1980s, a lot of research work on the seismic performance of masonry structures strengthened with FRP laminates has been carried out in China or elsewhere in the world, most of which were concerned with unreinforced masonry walls strengthened with CFRP or GFRP laminates. Velazquez et al. (2000) studied the failure modes and stress distribution of seven masonry walls strengthened with vertical GFRP laminates under out-of-plane loading. Prakash et al. (2008) studied the bearing capacity of masonry walls retrofitted by GFRP laminates based on experiments and conducted the numerical simulations of the walls on macro- and micro-levels using the software ABAQUS. Papanicolaou et al. (2011) compared the bearing and deformation capacity of masonry walls reinforced by CFRP, GFRP and BFRP laminates respectively under cyclic loading. Zhang et al. (2011) carried out shaking table test to investigate the seismic performance of a masonry structure strengthened with CFRP laminates. Xu et al. (2012) studied the dynamic characteristics and seismic responses of a masonry model strengthened with BFRP laminates through shaking table test, showing that the BFRP-strengthened masonry structure had a good capacity of seismic resistance.

To verify and compare the effectiveness of different retrofitting scheme for the masonry structure, two 1/4 scaled two-bay and two-storey masonry structures retrofitted by CFRP and BFRP laminates respectively were constructed in this study. The shaking table tests under various earthquake records were then conducted on the two specimens. The seismic responses of the two test models were obtained and compared.

2. TEST SPECIMEN

The test models were two-storey and two-bay masonry structures, which were adapted from masonry teaching buildings involving constructional columns. Considering the test condition, the length scale factor was set to be 1/4 and the elastic modulus scale factor was 1. To meet the requirement of additional mass, the acceleration scale factor was set to be 4. The other similarity ratios were derived from the above three basic similarity relations based on the theory of similarity, as listed in Table 2.1.

Table 2.1. Main Similarity Relations

Physical Quantities	Length	Acceleration	Elastic Modulus	Time	Destiny	Mass	Force
Scale Factor	1/4	4	1	1/4	1	1/64	1/16

Two test models strengthened with CFRP and BFRP laminates respectively were constructed, which was denoted as M1 and M2. The dimensions of the models were 1.850m × 1.425m × 1.500m (length × depth × height). As shown in the Figure 2.1, the walls located at the A-axis and the B-axis had door openings of 250mm × 525mm (width × height) and window openings of 375mm × 455mm (width × height) respectively. The walls were constructed on reinforced concrete foundation beams which were designed for convenience of lifting model. The angle irons were laid around the perimeter of foundation slab to anchor the test models onto the shaking table. The constructional columns with the section size of 60mm × 60mm were deployed at the intersection of the walls and the ring beams with the section size of 60mm × 60mm were located at every storey level. Slabs, constructional columns and ring beams were made by pisolite stone concrete and the steel reinforcements were represented by three types of galvanized iron wires whose areas were determined according to the laws of similitude. During the construction process, masonry walls were built firstly and then the constructional columns were constructed. The typical configuration and the field photo of one model are shown in Figure 2.1 and Figure 2.2 respectively. The measured mechanical properties of the materials used in the models are listed in Table 2.2.

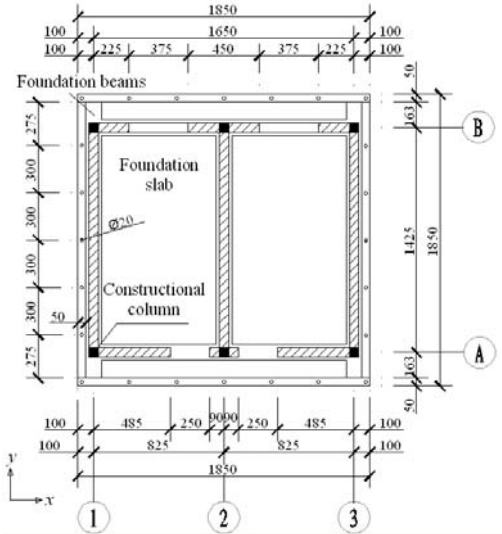


Figure 2.1. Typical configuration of the models (Unit: mm)



Figure 2.2. Photo of a model on the shaking table

Table 2.2. Measured Mechanical Properties Of Materials

Material	Destiny(kg/m ³)	Compressive strength(MPa)	Elastic modulus(MPa)
Concrete	2500	19.5	25115
Masonry	1932	4.4	1994

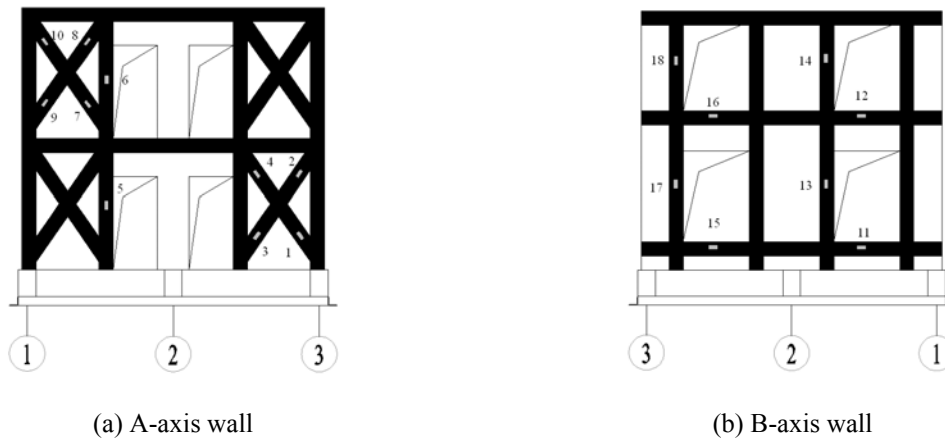


Figure 2.3. Reinforcement scheme

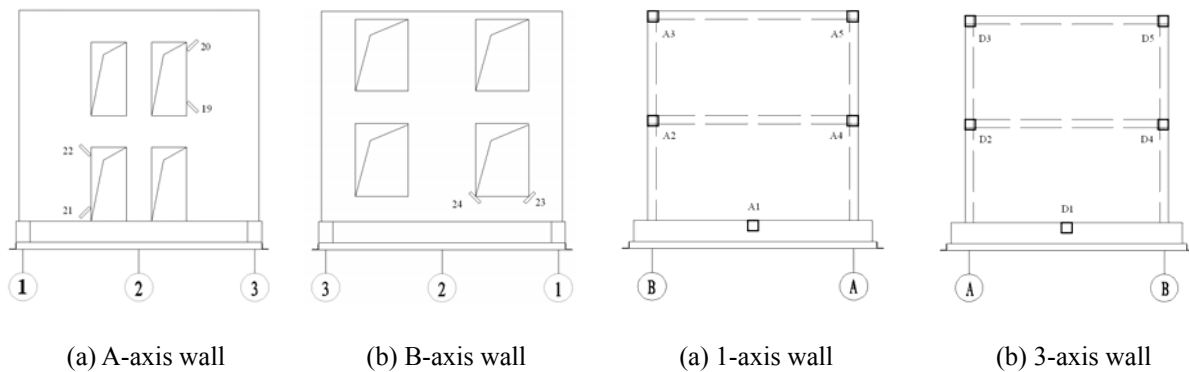


Figure 2.4. Arrangement of strain gauges on the inner side of walls

Figure 2.5. Arrangement of sensors ('A' and 'D' represent acceleration sensors and displacement sensors respectively)

The test models were reinforced along the x direction and therefore the FRP laminates with one layer were pasted outside the A-axis and B-axis walls, as seen in Figure 2.3, where the white rectangular blocks on FRP laminates represented strain gauges. The two models had the same layout of FRP laminates but with different FRP materials. The measured tensile strength and elastic modulus of CFRP laminates were 4363MPa and 241GPa, while BFRP laminates had the tensile strength of 1878MPa and the elastic modulus of 92GPa.

A total of 24 strain gauges were set on each model, among which 18 strain gauges were placed on the FRP laminates (see Figure 2.3 as mentioned above) and others were located on the inner side of walls (see Figure 2.4). As shown in Figure 2.5, five acceleration sensors and five displacement sensors were instrumented at the 1-axis wall and 3-axis wall respectively.

3. EARTHQUAKE INPUT

Base excitations were applied to each test model only in the x direction. Three earthquake records were selected including EL Centro record (1940, 180 components), Wenchuan record (2008, EW component) and Artificial record. As seen in Figure 3.1, the acceleration response spectra of the selected records matched well with the target spectrum pertaining to the frequent earthquake of intensity 7 according to the Chinese seismic design code (2010). Considering the requirements of similitude, the acceleration histories were scaled to be 4 times in acceleration axis and 25 percents in

time axis, as shown in Figure 3.2.

A total of 14 loading levels were applied to each model, in which EL Centro record, Wenchuan record and Artificial record were input in turn. As seen in Table 3.1, the peak acceleration of the first loading level was 0.1g and was increased by 0.1g for each level. In order to investigate the seismic responses under the frequent earthquake of intensity 7, the loading level with the peak acceleration of 0.15g was added. Before and after each loading level, the White Noise with the peak acceleration of 0.05g was applied to obtain the dynamic characteristics of each model, including frequency and damping ratio.

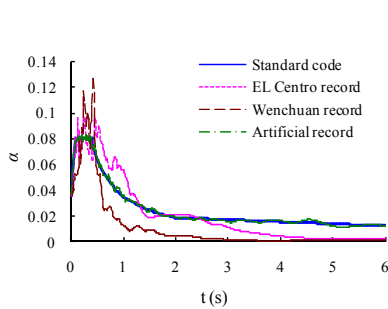


Figure 3.1. Acceleration response spectra

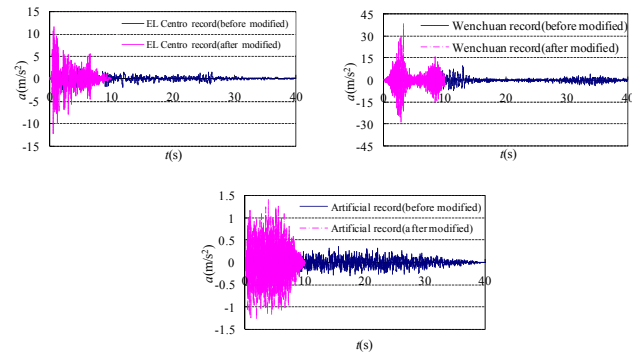


Figure 3.2. Base acceleration histories

Table 3.1. Typical Loading Level

Loading No.	Input Record	Peak Accel. /g	Loading level	Remark
1	White Noise	0.05		
2	EL Centro record	0.1	1	
3	Wenchuan record			
4	Artificial record			
5	White Noise	0.05		
6	EL Centro record	0.15	2	Frequent earthquake of intensity 7
7	Wenchuan record			
8	Artificial record			
9	White Noise	0.05		
18	EL Centro record	0.40	5	Design earthquake of intensity 7
19	Wenchuan record			
20	Artificial record			
21	White Noise	0.05		
38	EL Centro record	0.90	10	Rare earthquake of intensity 7
39	Wenchuan record			
40	Artificial record			
41	White Noise	0.05		
54	EL Centro record	1.30	14	
55	Wenchuan record			
56	Artificial record			
57	White Noise	0.05		

4. TEST RESULTS

4.1. Damage Pattern

After the seismic excitations, a number of cracks were observed on both models, as seen in Figure 4.1. It can be noticed as follows: (1) there are no cracks across brick, concrete and FRP laminates, meanwhile the bonding between FRP laminates and blocks did not fail; (2) the shear cracks appearing in x direction were distributed near FRP laminates; (3) the flexural cracks emerged in the y direction

for both models. A continuous horizontal crack was observed on the M2 model, which was not found on the M1 model.

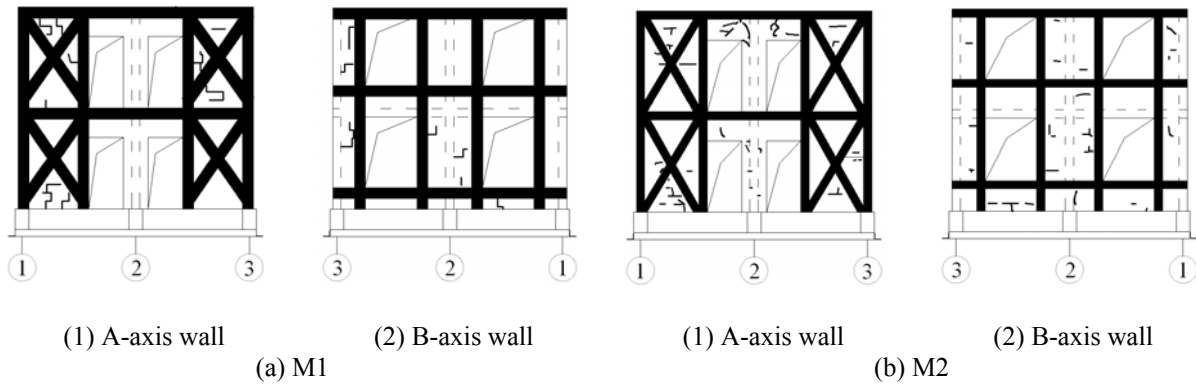


Figure 4.1. Crack patterns of the test models

During the first three loading levels, no cracking was observed on both of the models. The natural frequency of the M1 model remained nearly constant before the loading level corresponding to the frequent earthquake of intensity 7 with the peak acceleration of 0.15g, indicating that the M1 model worked in linear elastic condition. After the fourth loading level with the peak acceleration of 0.3g, little cracks were observed. Some vertical cracks also emerged to the left of door openings at the A-axis wall and the left of window openings at the B-axis wall. After the model was subjected to the design earthquake of intensity 7 with the peak acceleration of 0.4g, the existing cracks near the window openings at the B-axis wall extended and appeared to be stepped shape. At this time, its natural frequency dropped about 3%. Subsequently, with loading level increasing, existing cracks developed further along mortar joints and finally extended to foundation beams and ring beams. Under the loading level corresponding to the rare earthquake of intensity 7 with the peak acceleration of 0.9g, the cracks developed rapidly. When the peak acceleration went up to 1.3g, a step-shaped shear crack appeared in the y direction abruptly accompanied with horrible rupture sound. At last, the natural frequency of the M1 model decreased by about 26 per cent compared to the initial condition.

The M2 model remained elastic before the loading level pertaining to the frequency earthquake of intensity 7. When the peak acceleration increased to 0.3g, the horizontal cracks appeared near the left side of X-shaped BFRP laminates, the door openings at the A-axis wall and the window openings at the B-axis wall. A 50mm long horizontal crack emerged at the bottom of the 3-axis wall, and some step-shaped shear cracking appeared at the central region of the 1-axis wall. Under the loading level corresponding to the design earthquake of intensity 7 with the peak acceleration of 0.4g, some new cracks were observed near the left window openings of the B-axis wall and the bottom of the 3-axis wall. At this time the natural frequency decreased by about 5%. After the loading level corresponding to the rare earthquake of intensity 7 with the peak acceleration of 0.9g, more cracks emerged near BFRP laminates at the A-axis and the B-axis walls, the existing horizontal cracks in the y direction walls extended, and the natural frequency of the M2 model reduced about 14%. When the value of peak acceleration went up to 1.3g, the cracks developed more rapidly and the horizontal continuous crack at the 1-axis and 3-axis walls appeared. At ultimate, the natural frequency decreased more than 28 per cent.

4.2. Variation of Frequency

During the shaking table tests, dynamic characteristics of both models were also obtained. Before the shaking table test, modal tests were performed using the Hammer Method and the White Noise Method respectively, showing that: (1) using the Hammer Method, the first three model shapes for the M1 and M2 models were the same (see Figure 4.2), in which the first two modes translated in the x and y direction respectively and the third mode rotated along the z axis; the fundamental frequencies and the corresponding damping ratios of the two models were 34.3Hz (2.97%) and 33.5Hz (1.86%) respectively; (2) using the White Noise method, the fundamental frequencies and the corresponding

damping ratios of two models were 36.50 (0.79%) and 35.75 (0.782%); (3) a good match could be observed between the dynamic characteristics from the two methods, so the White Noise Method was adopted to obtain the dynamic characteristics of the test models for convenience.

The variations of natural frequencies of the two models are shown in Figure 4.3. It can be seen that before the design earthquake of intensity 7, the natural frequencies of the two models decreased nearly 5% compared to the original values. Subsequently, the natural frequencies dropped abruptly, especially after the rare earthquake of intensity 7. During the whole loading process, two platforms were observed on the variation curve of the natural frequencies of the M1 model, which can be attributed to the effect of CFRP laminates on improving structural stiffness. At last, the natural frequency of the M2 model declined more than 28%, a bit larger than that of the M1 model (26%). It could be concluded that CFRP laminates are more effective than BFRP laminates in terms of alleviating the structural stiffness degeneration, although the difference is not significant.

4.3. Amplification Effect

For each loading level, the Acceleration Dynamic Magnifications Factors (ADMF) at each storey level of the two models were computed. In this paper, the ADMF was defined as the ratio of the maximum acceleration response recorded at the storey level to the one at the base acceleration in the x direction. The responses at the storey level were obtained by averaging the recorded responses from the two acceleration sensors mounted the storey, as seen in Figure 2.5(a).

The variation of ADMFs of the two models under Wenchuan record are illustrated in Fig. 4.4, showing that: (1) under the same loading level, the ADMF of the second storey level was about two times that of the first one; (2) during the lower loading levels, the ADMFs of M1 were relatively higher than that of M2; however, with the loading level increasing, the ADMFs of the M1 model changed little while an obvious increase of ADMFs was observed for the M2 model. Fig. 4.5 shows the ADMFs of two models subjected to the loading level corresponding to the rare earthquake of intensity 7, it can be seen that a larger disparity existed between the ADMFs under different earthquake records for the M2 model compared to the M1 model.

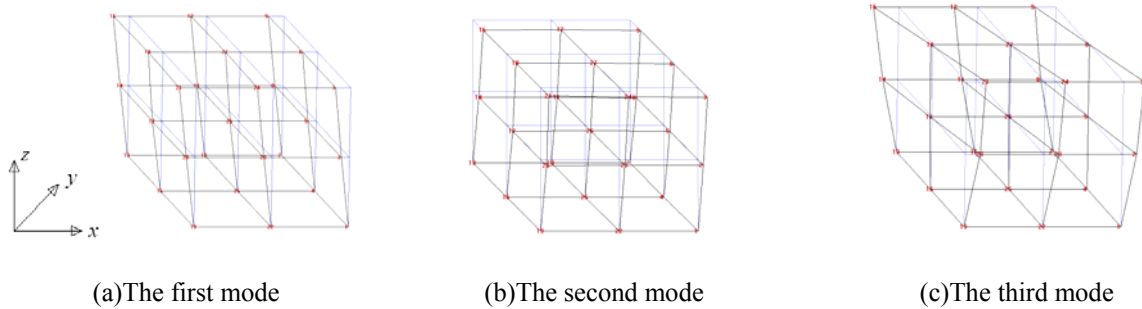


Figure 4.2. The first three mode shapes

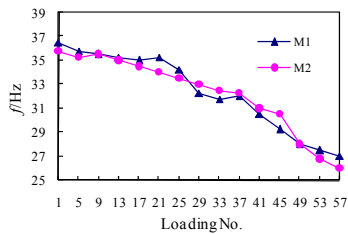


Figure 4.3. Variation of natural frequency

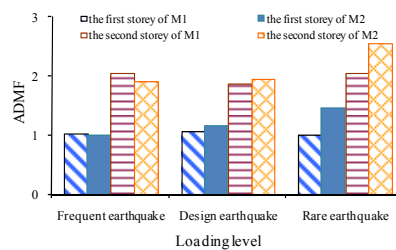


Figure 4.4. ADMF under Wenchuan earthquake record

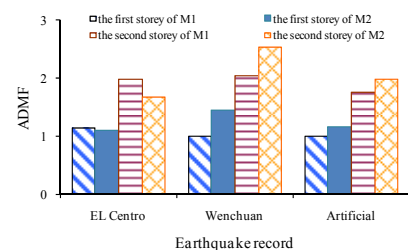


Figure 4.5. ADMF under rare earthquake of intensity 7

4.4. Displacement Response

As seen in Fig. 2.5(b), five displacement sensors were instrumented to record the absolute displacement at the story level of each model, among which D1, D2 and D3 were used to obtain the displacement of A-axis wall. The curves of relative displacement along the height for the two models under EL Centro are shown in Fig. 4.6. It could be seen that compared to the M2 model, with the loading level increasing, the increase of the relative displacement of the M1 model was much more obvious. The maximum relative displacements of the two models are 1.47mm and 1.22mm respectively. It could be also noted that during the loading process, the lateral displacement curves of the two models are both shearing type from beginning to end.

To investigate the torsion of the models, the displacement ratio was defined as the ratio of displacement at the two sides of models. According to the definition, the less torsion the model experienced, the value of displacement ratio is closer to 1. Figure 4.7 shows the displacement ratios of the two models under EL Centro record, from which it could be seen that torsion existed in the test models during the whole loading process. In the initial loading phase, the torsion occurred to the same degree in the two models. With the loading level increasing, the torsion effected on the M1 model changed little; however, for the M2 model, the torsion increased dramatically especially for the first storey. Overall, compared to the M2 model, the M1 model experienced less torsion, which can be evidenced by its displacement ratio closer to 1. Torsion mainly resulted from the following three aspects: (1) the geometry of the two models were unsymmetrical with bigger openings at the B-axis wall, leading to the comparatively lower stiffness of the B-axis wall; (2) the reinforcement scheme for the B-axis wall was different from that for the A-axis wall, as seen in Fig. 4.1; (3) the FRP laminate area of the A-axis wall was about 1.5 times that of the B-axis wall.

The relative displacement response of the two models subjected to different earthquake records with the loading level corresponding to rare earthquake of intensity 7 are shown in Figure 4.8. It can be seen that on the whole different earthquake records had slight influence on the displacement response, except for the displacement response at the second storey of the M1 model. For the M1 model, the maximum relative displacement of the first storey took place under Wenchuan record and the counterpart for M2 happened to Artificial record. For the second storey, the maximum relative displacements of the two models occurred under Artificial record and Wenchuan record respectively.



Figure 4.6. Relative displacement of the A-axis wall under EL Centro record

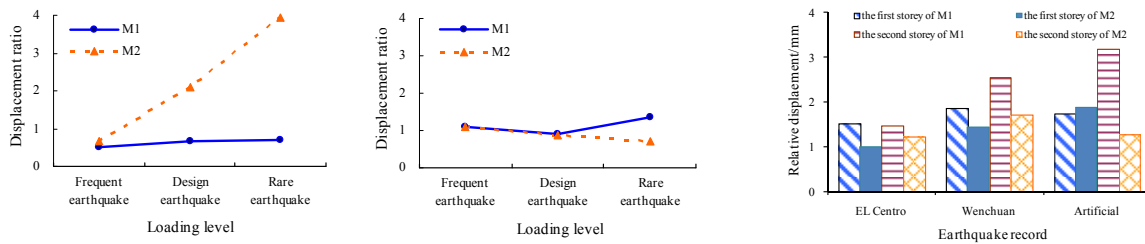
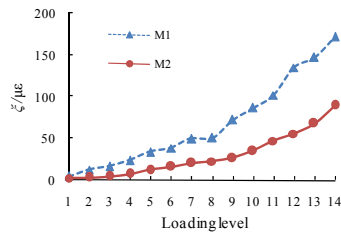
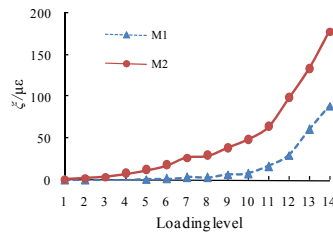


Figure 4.7. Displacement ratio under EL Centro record

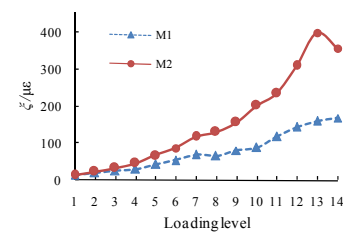
Figure 4.8. Relative displacement of A-axis wall under the rare earthquake of intensity 7



(a) point 8



(b) point 11



(c) point 24

Figure 4.9. Variation of strain

4.5. Variation of Strain

Most previous studies show that for the masonry walls strengthened with FRP laminates, the mechanic behavior of FRP laminates can be equivalent as the tie or strut in the truss model while the former plays the main role. In this section, the strain responses of three strain gauges were analyzed to investigate the mechanical behavior of the FRP laminates, among which point 8 and 11 strain gauges were arranged on FRP laminates (see Figure 2.3.) while point 24 strain gauge was located on the inner side of B-axis wall (see Figure 2.4(b)).

The variations of strain pertaining to the above three points with the increase of loading level are shown in Figure 4.9. From Figure 4.9(a), it could be seen that the maximum strain at point 8 of the CFRP laminates was $172\mu\epsilon$, about two times that of the BFRP laminates. From Figure 4.9(b), it could be seen that the strain values of BFRP remained at a low level until the crack near point 11 strain gauge occurred under the fourth loading level with the peak acceleration of $0.3g$, which indicates that similar to the CFRP laminates, the BFRP laminates started to work when crack appeared near the laminates. For point 11, the maximum strain of BFRP was $179\mu\epsilon$, much higher than that of CFRP. From Figure 4.9(c), it can be found that the disparity between the strains at the walls of the two models was little under initial loading levels; however, with the loading level increasing, the strain at point 24 of the M2 model reached $398\mu\epsilon$, about two times that of the M1 model. During the whole loading process, the maximum strain of CFRP and BFRP laminates were about $180\mu\epsilon$ and $400\mu\epsilon$, just about 1.24% and 2.17% respectively that corresponding to their design strength, which shows that FRP laminates did not work sufficiently, especially for the CFRP laminates.

5. CONCLUSION

In this paper, shaking table tests of two 1/4-scaled two-bay and two-storey masonry structures strengthened with CFRP and BFRP laminates respectively were conducted. Based on the test results, the seismic performance of the two retrofitted masonry structures was compared. The main findings are listed as follows:

- (1) Although a large number of shear cracks appeared in the models, no severe failure occurred on the structure level. The BFRP-strengthened model was damaged more seriously, indicating that the CFRP-strengthened one has a better seismic-resistant capacity.
- (2) The acceleration response of the CFRP-strengthened model changed little throughout the seismic loading while the BFRP-strengthened one increased significantly. The CFRP-strengthened model has a better deformation capacity and exhibited less torsion than the BFRP-strengthened one.
- (3) Both CFRP and BFRP laminates can effectively restrain the development of cracking, while the latter work more sufficiently with higher utilization ratio.
- (4) On the whole the masonry structure strengthened with CFRP laminates has comparable seismic performance to the one retrofitted by BFRP laminates. Considering its lower cost, the BFRP laminates

may have a good prospective in the applications of reinforcing masonry structures.

AKNOWLEDGEMENT

The authors are grateful to the People's Republic of China Housing and Urban-rural Construction Department for the research project (2010-1-154) and the Fundamental Research Funds for the Central Universities (2012210020205) for providing partial financial support. However, the opinions and conclusions expressed in this paper are solely those of the writers and do not necessarily reflect the views of the sponsors.

REFERENCES

- The People's Republic of China industry standards: JGJ116-2009 Technical specification for seismic strengthening of buildings. (2009). The People's Republic of China Housing and Urban-rural Construction Department. (In Chinese)
- Velazquez-Dimas J. I. and Ehsani M. R. (2000). Modeling out-of-plane behavior of URM walls retrofitted with fiber composites. *Journal of Composites for Construction*. **4:4**, 172-180.
- Prakash S. S. and Alagusundaramoorthy P. (2008). Load resistance of masonry wallets and shear triplets retrofitted with GFRP composites. *Cement & Concrete Composites*. **30**, 745–761.
- Papanicolaou C., Triantafillou T. and Lekka M. (2011). Externally bonded grids as strengthening and seismic retrofitting materials of masonry panels. *Construction and Building Materials*. **25**, 504-514.
- Ming-jie Zhang, Li-hua Xu, Si Zhang, Xiao-bin Hu. (2011). Shaking Table Tests of Seismic Performances of a Masonry Structure Retrofitted with CFRP Laminates. *Journal of civil engineering and management*. **28:3**, 89-93. (In Chinese)
- Li-hua Xu, Si Zhang, Xiao-bin Hu, Ming-jie Zhang. (2012). Dynamic properties and seismic responses of the masonry structure model strengthened with BFRP laminates. *2nd International Conference on Structures and Building Materials*, **446-449**, 3279-3286.
- Tianwen Wang. (2008). Civil Engineering Structural Test, Wuhan University of Technology Press, Wuhan, China. (In Chinese)
- The People's Republic of China industry standards: BG50003-2001 Code for design of masonry structures. (2001). The People's Republic of China Construction Department. (In Chinese)